Polypyrrole as Conducting Polymer Coating on Ti6Al7Nb Alloy

MIHAELA MINDROIU[1], CRISTIAN PIRVU[1], SIMONA POPESCU[1], IOANA DEMETRESCU[1]*

[1] Politehnica University of Bucharest, Faculty of Applied Chemistry and Materials Science, 1-7 Polizu Str., 011061, Bucharest, Romania

Conducting polymer coating has been used to improve the surface performance of metallic materials, as Ti6Al7Nb alloy. Polypyrrole (PPy) was electrochemically deposited from 0,2 M oxalic acid aqueous monomer solutions by three different methods: potentiostatic, galvanostatic and potentiodynamic techniques. The stability of PPy / Ti-6Al-7Nb surface has been studied by electrochemical methods in Hank's Balanced Salt Solution (HBSS) by Tafel tests and cycle voltammetry. The PPy / Ti-6Al-7Nb biofluid interface was analysed by electrochemical impedance spectroscopy (EIS) and the corresponding equivalent circuits were proposed. The structural infrared analysis and morphology of conducting polymer layer on titanium alloy have been evaluated.

Keywords: Polypyrrole, Ti6Al7Nb alloy, stability properties, EIS, AFM

Today, an important approach regarding improving metallic materials performance as corrosion and wearing resistance [1], conductivity, biocompatibility [2] is covering alloys with polymer thin layers. The procedures that aim at such improvement are frequently related to electrochemical methods and various electrodeposition systems with polymers were reported in the last decade [1, 3], as neural tissue electrode [4] for long term implant. Pyrrole and its derivatives yield an important class of electronically conducting polymers that could be promising candidates as implant substrates modifiers. Polypyrrole can be prepared via chemical or electrochemical polymerization [5]. The latter is generally preferred because it provides a better control of film thickness and morphology. Different electropolymerization techniques can be used including potentiostatic (constant-potential), galvanostatic (constant current) and potentiodynamic (potential scanning *i.e.* cyclic voltammetry) methods.

Polypyrrole films deposited on Ti6Al7Nb substrates could be used to graft biologically active molecules which accelerate the process of osseointegration [6-8] and to protect the surface of the substrate from corrosion [9, 10]. Polypyrrole has also been used as an active component of bilayer or multilayer strips in artificial muscles [11].

The aim of this paper was to improve the surface performance of biomaterials based on titanium alloy by electrodeposition of polypyrrole by potentiostatic, galvanostatic and potentiodynamic techniques.

Experimental part

The substrates were represented by Ti-6Al-7Nb alloy with composition given in table 1. All experiments were carried out on disk-shaped samples (1 cm diameter, 2 cm thickness). Their surface was polished to a finish (Ra =1 μm) with 1200 silica carbide paper and rinsed well with distilled water before performing the electrodeposition experiments.

The polypyrrole films were synthesized electrochemically from aqueous solution containing 0,1 mol L^{-1} Py and 0,2 mol L^{-1} oxalic acid as support electrolyte, using three different techniques. In the first procedure, potentiodynamical method, the working electrode potential was cycled between 0 to 1.1 V for 5 cycles, at a scan rate of 50 mV s^{-1}, while in the second procedure the electrode was maintained under potentiostatic conditions for 500 seconds at 0.9 V .In the third procedure, the electrode was maintained under galvanostatic conditions for 500 seconds at 90 μA.

Pyrrole (Py) monomer was purchased from Aldrich, distilled and stored in the dark at -20°C prior to use.

Corrosion measurements were performed in aerated simulated physiological HBSS [12] containing (in gL^{-1}): 8 NaCl, 0.4 KCl, 0.35 $NaHCO_3$, 0.25 $NaH_2PO_4 \cdot H_2O$, 0.06 $Na_2HPO_4 \cdot 2H_2O$, 0.19 $CaCl_2 \cdot 2H_2O$, 0.19 $MgCl_2$, 0.06 $MgSO_4 \cdot 7H_2O$, 1 glucose, at *p*H = 6.9.

All electrochemical measurements, such as electrochemical deposition, electrochemical characterization and EIS investigation, were performed using a one compartment cell with three electrodes: a working electrode, a platinum counter-electrode and an Ag/AgCl, KCl reference electrode connected to Autolab PGSTAT 302 N potentiostat with NOVA general-purpose electrochemical system software.

The Fourier transform infrared (FT-IR) spectroscopic analysis for electrodeposited polypyrrole films was done by 100 Perkin Elmer equipment using diamond ATR technique.

The surface analysis and roughness evaluation were performed using an electrochemical atomic force microscope (AFM) from APE Research, Italia.

Results and discussion

Electrochemical deposition of polypyrrole coating

Potentiodynamic polymerization of pyrrole

Figure 1 presents the first five cycles of the voltammograms obtained on Ti6Al7Nb electrode in 0,2 M oxalic acid aqueous solution (fig. 1 a) and in 0,1 mol L^{-1} pyrrole in 0,2 M oxalic acid aqueous solution (fig. 1 b).

Element	Ti	Al	Nb	Fe	H	N	O	C
(wt% values)	rest	5.88	6.65	0.3	0.0121	0.05	0.2	0.1

Table 1
COMPOSITION OF THE Ti-6Al-7Nb ALLOY

* *email: i_demetrescu@chim.pub.ro*

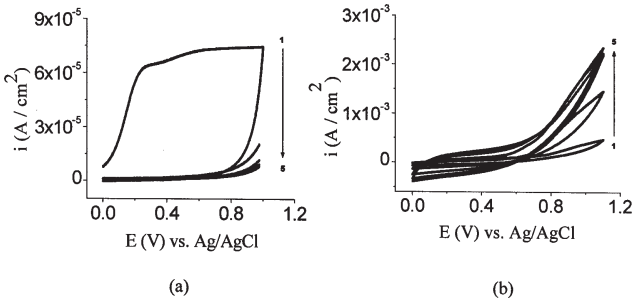

Fig. 1. Cyclic voltammograms obtained on Ti6Al7Nb electrode in 0.2 M oxalic acid aqueous solution (a) and in 0.1 mol L^{-1} pyrrole in 0.2 M oxalic acid aqueous solution (b), scan rate of 50 mV/s

The first anodic branch of titanium alloy in oxalic acid solution (fig. 1 a) starts with a suddenly increase of the current density corresponding to complex oxidation reaction onto the electrode surface. Therefore, the potentiodynamic curves recorded at a scan rate of 50 mVs^{-1} present in the first cycle a large plateau of about 800 mV followed by a drastically decrease of the current on the successive sweeps. The formed passive layer inhibits further oxidation of titanium alloy and the electrode surface is practically blocked after the second cycle.

Figure 1b, corresponding to potentiodynamic polymerization of pyrrole in 0.2 M oxalic acid aqueous solution presents a gradually increase of the current density in the successive cycles showing a polymerization of pyrrole. Also, the steadily rising capacitive behaviour of the new obtained PPy / Ti6Al7Nb can be observed on the 0 – 0.7 V. The obtained films are black, homogeneous and adherent to the electrode surface.

Potentiostatic polymerization of pyrrole

The electrosynthesis of PPy films on Ti6Al7Nb electrode can be also performed by the potentiostatic technique, in one potential step, by applying 0,9 V vs. Ag/AgCl.

The current transient obtained for a typical potentiostatic PPy electrodeposition, presented in figure 2, can be divided into two stages: at the beginning, the current density decreased during to electrode passivation due to oxide layer formation; in the second stage the polymer nucleation is started, and in the third stage the current density plateau of about 5 $\mu A/cm^2$ can be observed corresponding to the polymer electrodeposition.

The total charge used for potentiostatic polymerization of Py in 0,2 M oxalic acid aqueous solution is 94 mC.

Galvanostatic polymerization of pyrrole

Figure 3 shows growth of a PPy film on Ti6Al7Nb electrode by galvanostatic electrodeposition at the applied current of 90 µA in 0.2 M oxalic acid aqueous solution. The start potential salt after applied anodic current is about 800 mV.

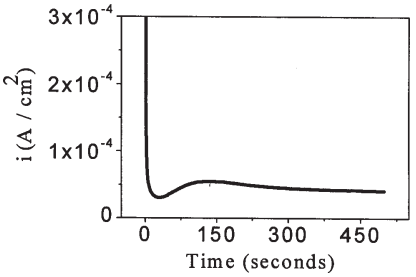

Fig. 2. Chronamperometric curves during potentiostatic electrodeposition from 0.1 mol L^{-1} pyrrole in 0.2 M oxalic acid aqueous solution on a Ti6Al7Nb electrode at the applied 0.9 V.

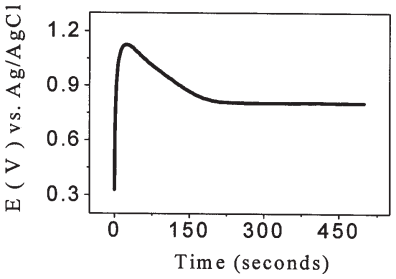

Fig. 3. Electropolymerisation by galvanostatic electrodeposition from 0.1 mol L^{-1} pyrrole in 0.2 M oxalic acid aqueous solution on a Ti6Al7Nb electrode at the applied current of 90 µA.

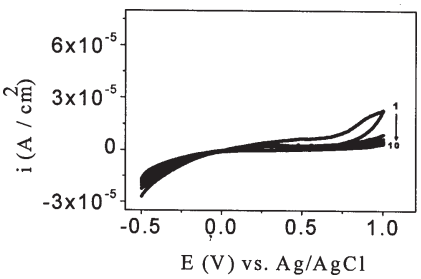

Fig. 4. Cyclic voltammograms for uncoated TiAlNb electrode in Hank solution, scan rate 0.05 V/s, 10 cycles

The polymerization potential plateau is stabilized at 0.8 V which is almost similar with the value of the starting monomer oxidation potential from the recorded cyclic voltammogram.

Electrochemical and corrosion resistance characterization

Cyclic voltammetry

Cyclic voltammograms recorded for uncoated titanium alloy in Hank solution, figure 4, show an oxidation part in the first cycle followed by the passivation in the next cycles.

For PPy coated titanium alloy in Hank solution the surface presents a capacitive behaviour, especially for PPy potentiodymically deposited, (fig. 5). Also, the PPy coating shows a good electrochemical stability, especially for potentiodymically deposited coatings where the successive ten cycles are practically overlaid.

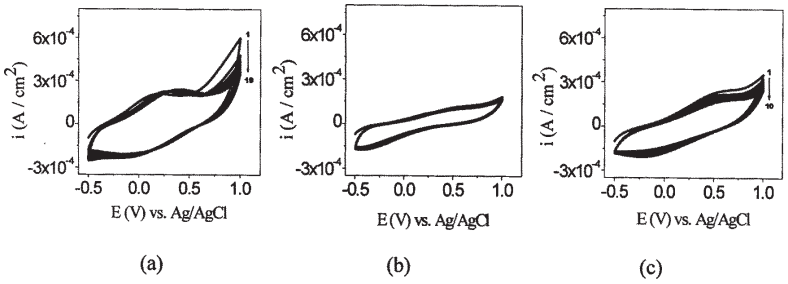

Fig. 5. Cyclic voltammograms for (a) TiAlNb/PPy potentiodymically deposited; (b) TiAlNb/PPy potentiostatically deposited; (c) TiAlNb/PPy galvanostatically deposited -0.5-1V, 0.05V/s, 10 cycles

Table 2
CORROSION PARAMETERS OBTAINED FROM TAFEL DIAGRAMS

Parameters	Uncoated Ti6Al7Nb	Ti6Al7Nb / Ppy Potentiostatic	Ti6Al7Nb / Ppy potentiodynamic	Ti6Al7Nb / Ppy galvanostatic
I_{cor} (A/cm^2)	$1.016 \cdot 10^{-6}$	$2.108 \cdot 10^{-6}$	$2.375 \cdot 10^{-6}$	$7.033 \cdot 10^{-6}$
E_{cor} (V)	-0.065	0.08	0.072	-0.004
Rp (Ohm)	$2.283 \cdot 10^{+4}$	$4.184 \cdot 10^{+3}$	$3.553 \cdot 10^{+3}$	$4.032 \cdot 10^{+2}$
V_{cor} (mm/year)	$9.20 \cdot 10^{-3}$	$5.913 \cdot 10^{-2}$	$6.66 \cdot 10^{-2}$	$1.972 \cdot 10^{-1}$

A very good stability of PPy / titanium alloy surface creates the perspectives of using to sensor and biosensor application.

Tafel plots

The corrosion behaviour of uncoated and coated Ti6Al7Nb alloys electrodes was estimated by Tafel curve in HBSS. The Tafel regions of cathodic and anodic polarization curves are extrapolated. Figure 6 shows the set of polarization curves recorded for uncoated and coated Ti6Al7Nb alloys electrode in Hank solution.

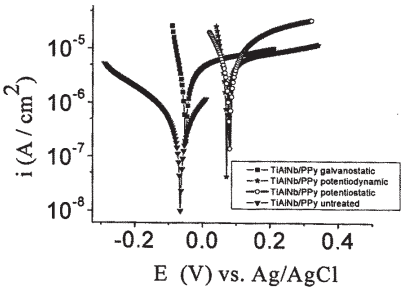

Fig. 6. Tafel diagrams for uncoated and electrochemically modified by PPy films obtained from 0.2 M acid oxalic on Ti6Al7Nb electrodes in HBSS

Comparing the plots obtained both on uncoated and coated Ti6Al7Nb surfaces in Hank solution it could be seen an apparently better anti-corrosion behaviour for uncoated titanium alloy reflected by better corrosion parameters.

However, the presence of PPy coating on the titanium alloy surface brings an anodic shift of the corrosion potential with about 150 mV. The ten time higher corrosion current for coated titanium alloy can be attributed to conducting surface of the PPy comparing with non-conducting oxide natural growth surface of titanium alloy.

For PPy coated Ti6Al7Nb alloy the better anti-corrosion behaviour in Hank solution was observed for potentiostatic and potentiodynamic growth coatings.

In table 2 are presented corrosion parameters and polarisation resistances obtained from Tafel diagrams.

Electrochemical impedance spectroscopy

EIS analysis was discussed in term of Bode and Nyquist representations. Nyquist spectra for uncoated electrode and electrochemical modified by PPy films are presented in the figure 7. In all cases the impedance spectra were achieved at free potential in Hank solution.

For bulk titanium alloy surface, a single time constant with solution resistance, Rs, and charge transfer resistance, R_1 and constant phase element, Q_1, were proposed (fig. 7 a). For Ti6Al7Nb / PPy surface in Hank solution we found another circuit with a supplementary constant phase element, Q_2, corresponding to the PPy film (fig. 7 b).

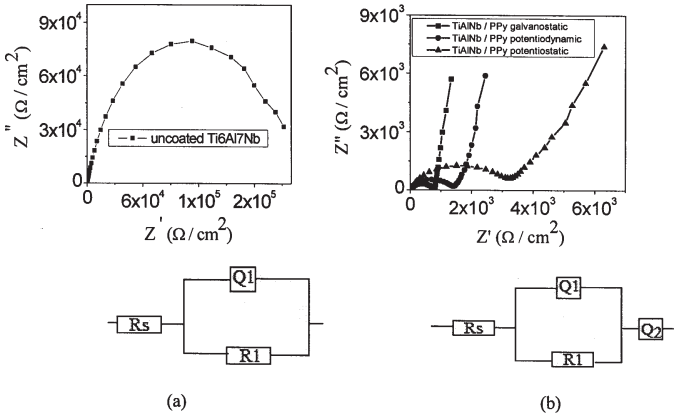

Fig. 7. Nyquist spectra for uncoated Ti6Al7Nb alloy (a) and Ti6Al7Nb electrodes electrochemical modified by PPy films obtained from 0.2 M oxalic acid (b) in Hank solution.

For the description of a frequency independent phase shift between an applied AC potential and its current response, a constant phase element (CPE) was used.

The electrical parameters obtained after fitting of proposed circuits are in the table 3.

The charge transfer resistance from obtained EIS data is in concordance with the polarization resistance values from Tafel plots: $3.22 \cdot 10^{+3}$ Ω and $4.184 \cdot 10^{+3}$ Ω for potentiostatically deposited PPy, $1.40 \cdot 10^{+3}$ Ω and $3.553 \cdot 10^{+3}$ Ω for potentiodinamically deposited PPy and $7.64 \cdot 10^{+2}$ Ω and $4.032 \cdot 10^{+2}$ for galvanostatically deposited PPy, respectively.

Surface characterization

Infrared characterization

The scanning was ranged from 4000 cm^{-1} to 600 cm^{-1}. The FT-IR absorption spectra of PPy, presented in figure 8, show a quasi similar aspect.

From all PPy depositions on Ti6Al7Nb electrode it can be observed that the NH stretching band of pyrrole ring appears at 3407.54 cm^{-1} in galvanostatic technique,

Table 3
ELECTRICAL PARAMETERS AFTER EIS DATA FITTING

Parameters	Ti6Al7Nb uncoated	Ti6Al7Nb / Ppy Potentiostatic	Ti6Al7Nb / Ppy Potentiodynamic	Ti6Al7Nb / Ppy Galvanostatic
R_{sol} (Ω)	57.2	22.26	15.76	13.68
CPE 1(F)	$0.6241 \cdot 10^{-5}$	$0.8932 \cdot 10^{-5}$	$0.6278 \cdot 10^{-5}$	$0.6528 \cdot 10^{-5}$
n 1	0.808	0.8251	0.8688	0.9015
R_{ct} (Ω)	$2.14 \cdot 10^{+5}$	$3.22 \cdot 10^{+3}$	$1.40 \cdot 10^{+3}$	$7.64 \cdot 10^{+2}$
CPE 2 (F)		$0.9278 \cdot 10^{-3}$	$0.1767 \cdot 10^{-2}$	$0.2397 \cdot 10^{-2}$
n 2		0.7175	0.8382	0.9314

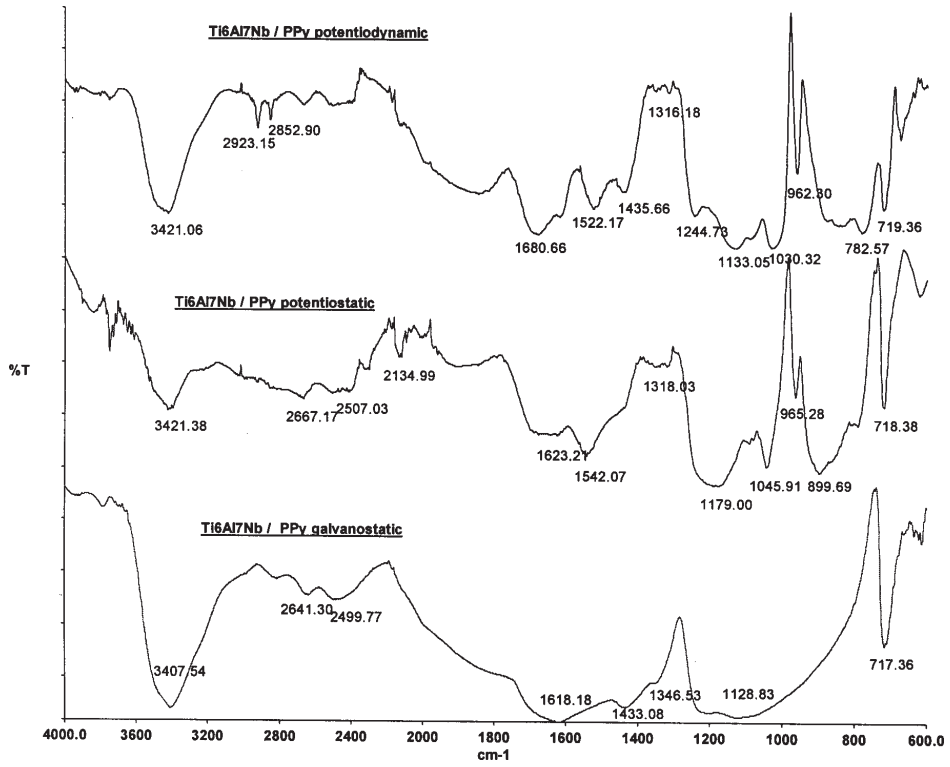

Fig. 8. FT-IR spectra of PPy films electrodeposited in oxalic acid aqueous solution.

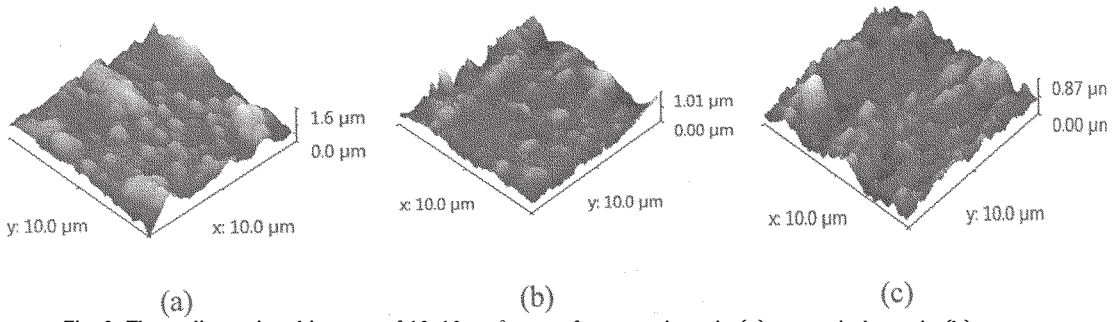

(a) (b) (c)

Fig. 9. Three-dimensional images of 10x10 μm^2 scans for potentiostatic (a), potentiodynamic (b), and galvanostatic (c) polymerized of Py in acid oxalic 0.2M aqueous electrolyte.

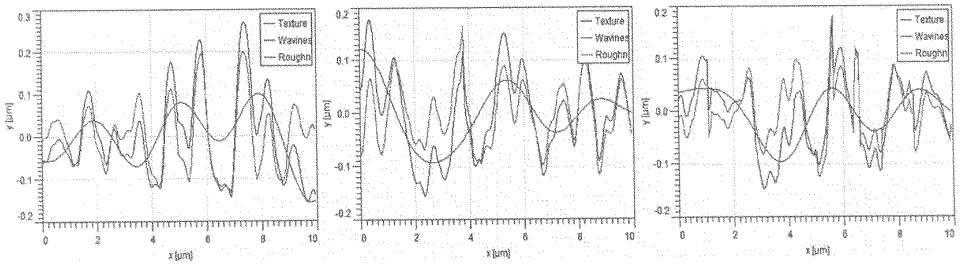

(a) (b) (c)

Fig. 10. Roughness parameters (texture, waviness, roughness) for potentiostatic (a), potentiodynamic (b), and galvanostatic (c) polymerized of Py in acid oxalic 0.2M aqueous electrolyte

3421.38 cm^{-1} in potentiostatic deposition and 3421.06 cm^{-1} respectively in potentiodynamic method.

The stretch vibration of C-H bond [13] appears weakly between 2930 - 2000 cm^{-1}.

The characteristic PPy absorption bands at 1600-1100 cm^{-1} are more accentuated in case of potentiostatic and potentiodynamic deposition than in galvanostatic method. The spectum of PPy obtained by potentiodinamic method presents at 1680.66 cm^{-1} band absorption assigned to the C = O stretch vibration from acid oxalic. On the other hand, in case of spectra for PPy obtained by potentiostatic and galvanostatic methods, the absorption bands at 1623.21 cm^{-1} and 1618.18 cm^{-1} respectively correspond to the C=C ring stretching of pyrrole. The typical PPy ring fundamental N-H vibrations were observed at 1522.17 cm^{-1} and 1435.66 cm^{-1} in spectrum Ti6Al7Nb / PPy potentiodynamic, at 1542.07 cm^{-1} in spectrum Ti6Al7Nb / PPy potentiostatic and at 1433.08 cm^{-1} in spectrum Ti6Al7Nb / PPy galvanostatic [14]. The peaks at 1128.83 cm^{-1}, 1179 cm^{-1} and 1133 cm^{-1} are due to C-C stretching. The spectra Ti6Al7Nb / PPy potentiodynamic and Ti6Al7Nb / PPy potentiostatic present at 1045.91 cm^{-1} and at 1030.32 cm^{-1} absorption bands corresponding to the =C-H in plane vibration [15]. These bands are not observed in Ti6Al7Nb / PPy galvanostatic spectrum.

Table 4
ROUGHNESS FOR THE SURFACE OF UNCOATED AND Ti6Al7Nb / PPy ELECTRODS

Electrods	R_a (μm)	R_{ms} (μm)
Uncoated Ti6Al7Nb	0.0165	0.0193
Ti6Al7Nb / PPy potentiostatic	0.189	0.231
Ti6Al7Nb / PPy potentiodynamic	0.137	0.180
Ti6Al7Nb / PPy galvanostatic	0.0438	0.0546

Also, the peaks observed at 962.30 cm^{-1} and 965.28 cm^{-1} out of C-C stretching are observed only in case of potentiodynamic and potentiostatic deposition methods. In all deposition cases is observed the =C-H out of plane vibration at 719.36 cm^{-1}, 718.38 cm^{-1} and at 717.36 cm^{-1}, indicating the polymerization of pyrole [14].

Surface analysis with Atomic Force Microscopy

In order to investigate the surface topography of PPy modified surfaces the contact mode Atomic Force Microscopy (AFM) was used.

Figure 9 shows three-dimensional images of 10x10 μm scans for potentiostatic (a), potentiodynamic (b) and galvanostatic (c) polymerized PPy in oxalic acid aqueous solution.

The texture of the all PPy coated titanium surface shows the presence of the large grain around 1 μm which is well definite especially for potentiostatic and potentiodynamic coatings, according to figure 10. The surface waviness shows a quasi similar behaviour for all kinds of coating.

The PPy roughness is higher for potentiostatic deposition than that obtained by potentiodynamic and galvanostatic deposition, as can be seen in table 4.

The roughness is smaller in the case of uncoated alloy.

Conclusions

The PPy coating obtained by potentiostatic method was found to have better properties like conductive and protective layer.

The charge transfer resistance from obtained EIS data is in concordance with the polarization resistance values from Tafel plots showing a better resistance for potentiostatically deposited PPy.

The FT-IR spectroscopic analysis for films electro-deposited from aqueous oxalic acid solution indicated the polymerization of pyrrole.

Acknowledgements: The authors gratefully acknowledge the support of the Romanian National CNCSIS Grant IDEI COMPLEXE No. 248 / 2008

References

1. CORABIERU, P., VELICU, S., CORABIERU, A., VASILESCU, D., VODA, M., Mat. Plast., **46**, no. 1, 2009, p. 16
2. GUIMARD, N. K., GOMEZ, N., SCHMIDT, C. E., Prog. Polym. Sci., **32**, 2007, p. 876
3. OBREJA, L., DOROHOI, D., MELNIG, V., FOCA, N., NASTUTA, A., Mat. Plast., **45**, no. 3, 2008, p. 261
4. GREEN, R. A., LOVEL, N. H., WALLACE, G. G., POOLE –WARREN L. A., Biomaterials, **29**, 2008, p. 3393
5. SAIDKI, S., SCHOTTLAND, P., BRODIE, N., SABOURAUND, G., Chem. Soc. Rev., **29,** 2000, p. 283
6. GIGLIO, E. D. E., GUASCITO, M. R., SABBATINI, L., ZAMBONIN, P., Biomaterials, **22**, 2001, p. 2609
7. DING, L., HAO, C., ZHAHG, X., JU, H., Electrochemistry Communications, **11**, 2009, p. 760
8. MEKHALIF, Z., COSSEMENT, D., HEVESI, L., DELHALLE J., Applied Surface Science, **254**, 2008, p. 4056
9. MARTINS, N. C. T., MOURA, E., SILVA, T., MONTEMOR, M. F., FERNANDES, J. C. S., FERREIRA, M. G. S., Electrochimica Acta, **53**, 2008, p. 4754
10. ARENAS, M. A., BAJOS, G. L., DAMBORENEA, J. J., OCÓN, P., Progress in Organics Coatings, **62**, 2008, p. 79
11.SKOTHEIM, T. A., REYNOLDS, J. R., Handbook of Conducting Polymers, Conjugated Polymers – Processing and Applications, 3 edition, Taylor & Francis Group, Edited by Torje A. Skotheim and John R. Reynolds, New York, 2007, p. **11**-21
12. METIKOS –HUKOVIC, M., KWOKAL, A., PILJAC, J., Biomaterials, **24**, 2003, p.3765
13.YEE, L. M., KASSIM, A., MAHMUD, H. N. M. E., SHARIF, A. M., HARON, M. J., The Malaysisn Jurnal of Analytical Sciences, **11**, no. 1, 2007, p.133
14. VISHNUVARDHAN, T.K., KULKARNI, V.R., BASAVARAJA, C., RAGHAVENDRA, S.C., Bull. Mater. Sci., **29**, nr. 1, 2006, p.77
15. LU, X. F., CAO, D. M., CHEN, J., ZHANG, W J., WEI, Y., Mater Lett, **60**, 2006, p.2851

Manuscript received: 22.07.2009